INSTITUTE OF PHYSICS PUBLISHING PHYSICS IN MEDICINE AND BIOLOGY

Phys. Med. Biol. **47** (2002) 3823–3830 PII: S0031-9155(02)39036-5

Scale model experimentation: using terahertz pulses to study light scattering

Jeremy Pearce and Daniel M Mittleman

Department of Electrical and Computer Engineering, MS 366, Rice University, Houston, TX 77251-1892, USA

E-mail: daniel@rice.edu

Received 19 February 2002
Published 17 October 2002
Online at stacks.iop.org/PMB/47/3823

Abstract

We describe a new class of experiments involving applications of terahertz radiation to problems in biomedical imaging and diagnosis. These involve scale model measurements, in which information can be gained about pulse propagation in scattering media. Because of the scale invariance of Maxwell's equations, these experiments can provide insight for researchers working on similar problems at shorter wavelengths. As a first demonstration, we measure the propagation constants for pulses in a dense collection of spherical scatterers, and compare with the predictions of the quasi-crystalline approximation. Even though the fractional volume in our measurements exceeds the limit of validity of this model, we find that it still predicts certain features of the propagation with reasonable accuracy.

1. Introduction

The applications of terahertz science and technology to problems in medicine and biology have so far generally fallen into two classes. The first class consists of spectroscopic measurements of biological or biochemical systems, including DNA, proteins, and other biologically relevant molecular species [1–3]. The second involves imaging of biological materials, such as for example teeth, skin or excised tissue samples [4–7]. Numerous examples of both these classes can be found elsewhere in this special issue. In this paper, we describe a third type of measurement for which terahertz time-domain spectroscopy (THz-TDS) is uniquely suited, and for which several opportunities exist in the biological and medical sciences. This third class of measurement is based on the idea of using scale models to elucidate the physics of wave propagation and scattering. One can readily study a simplified, well-controlled model of millimetre dimension. Then, because of the invariance of Maxwell's equations to length, one can scale these results to either larger or smaller dimension and thus provide insight and guidance for researchers working at other wavelengths [8]. Cheville and Grischkowsky have recognized the power of THz-TDS for scale model experimentation in measurements which

simulate broadband radar [9]. We have recently used related techniques for scaled studies of acoustic pulse propagation in geophysical strata [10]. In this paper, we discuss the possibility of scaling in the opposite direction, to smaller rather than larger targets, as a method for understanding optical pulse propagation in complex media.

The types of problems for which such techniques are likely to be useful include the study of free-space propagation in strongly scattering media, such as biological tissue. The problem of light propagating in biological media has been the subject of great attention for many years, due to the potential for using optical methods as imaging diagnostics. Because of the random nature of tissue optical properties, this problem is very challenging. In a random or turbid medium, transmitted radiation consists of a coherent, unscattered wave superimposed on an incoherent wave consisting of photons which have scattered one or more times. Both the coherent [11, 12] and incoherent [13, 14] portions have been used to form images of various properties of the medium. Despite these impressive results, many fundamental questions remain unanswered. For example, even for the ballistic (unscattered) radiation, for which one might suppose the situation is the simplest, the correct method for computing the values of the effective propagation constants at high scatterer density is a topic of current research [15–18]. Experimental and theoretical studies to elucidate this issue have been pursued for many years [19–23].

As a first demonstration of the utility of THz scale model experimentation, we study the ballistic transport of THz pulses through dense distributions of spherical scatterers [24]. Many previous experiments on this subject have employed radiation at optical frequencies. In this case, it is relatively easy to obtain the imaginary part of the effective propagation constant, but interferometric techniques are required to extract the real part [17]. Terahertz spectroscopy affords easy access to both the real and imaginary parts, providing a wealth of additional information. In addition, many previous measurements have been based on single-frequency or narrow-band measurements, for which the size parameter of the scatterers is approximately constant. In contrast, THz-TDS is inherently a broadband technique. With this source, one can perform measurements which span the entire range from Rayleigh scattering ($ka \ll 1$, where k is the free-space wave vector and a is the particle diameter) through Mie scattering ($ka \geqslant 1$), and thus fully characterize the propagation. In addition, a continuous broadband source is required in order to characterize parameters such as the group velocity, which depend on derivatives of the effective refractive index. Previous researchers have exploited these advantages in the microwave regime [21]. A final advantage of THz measurements involves the preparation of the samples. In optical experiments, the most common model scattering medium is a suspension of latex spheres in water, for which characterization of the density and the size distribution is not straightforward. Sample preparation and characterization are not significant issues in the THz domain.

2. Experimental method

Because we are interested in the propagation of the ballistic (unscattered) radiation, the experimental configuration is quite simple. The sub-picosecond THz pulses are generated and detected using a set-up quite similar to those described previously [25, 26], except that $f = 10$ cm polyethylene lenses are used instead of off-axis paraboloidal reflectors to transport the THz beam, as shown in figure 1. The confocal parameter for our optical configuration is at least ten times the sample thickness, so the beam approximates a plane wave in the medium. We construct a model random medium using commercially available polytetrafluoroethylene (PTFE, teflon) spheres, with size polydispersity $<3\%$ on the diameter. Teflon is an excellent material for these studies since its absorption coefficient is quite low at terahertz frequencies.

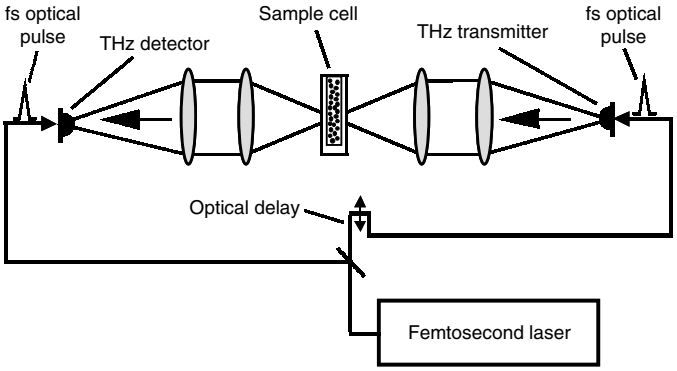

Figure 1. A schematic of the transmission experiment.

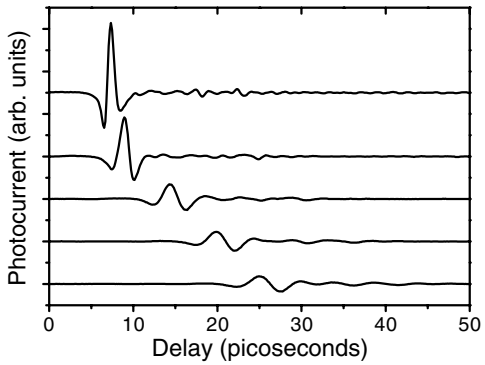

Figure 2. The upper waveform is a typical reference, transmitted through an empty cell. The subsequent four waveforms illustrate the decreasing transmission and increasing delay with increasing optical path length through the scattering medium. The path lengths for these data are 1.59, 7.94, 14.29 and 20.64 mm.

Also, the refractive index of teflon, $n_{\mathrm{PTFE}} = 1.4330$, is nearly independent of frequency throughout the spectral range of the measurements [27]. We have studied spheres of 0.794 mm diameter. The spheres are contained in a teflon sample cell, with windows a fixed distance apart. In order to perform length-dependent studies, we fabricated 50 such cells, with internal path lengths ranging from 1.19 mm to 20.64 mm. We determine the number density of spheres n_0 by weighing each cell on a precision balance. From such measurements we determine a number density of $n_0 = 2.14 \pm 0.15$ spheres per mm^3, and therefore a volume fraction of $\phi = 0.56 \pm 0.04$.

For each path length, we collect both a reference (empty cell) and a sample waveform, to correct small variations in the thickness of the cell windows. Figure 2 shows a series of THz waveforms, for several different path lengths. As the path length increases, the pulses take longer to transit through the sample, and their amplitude decreases. This decrease is primarily due to the scattering of high-frequency components. From this data, we can extract the frequency-dependent reduced scattering coefficient μ_s' using the Fourier transform of the measured time-domain waveforms [24]. Because the THz fields are measured coherently, we can also determine the effective refractive index n_{eff} of the scattering medium from the phase of the Fourier transform. This effective index can differ quite substantially from a

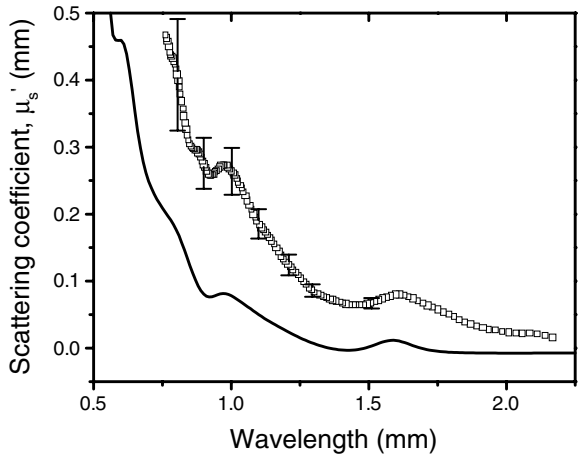

Figure 3. The open squares show the measured reduced scattering coefficient as a function of wavelength, extracted from the time-domain waveforms by Fourier transform. The error bars show typical uncertainties due to variability in repeated measurements. The solid curve shows the prediction of the quasi-crystalline approximation.

simple volume-weighted average index, as a result of interference between multiple scattered waves [28].

3. Analysis and discussion

Numerous theoretical models have been used to compute these effective propagation parameters for waves in dense collections of scatterers. These models are generally based on the multiple scattering equations, a system of equations relating the field incident on a particular scatterer to the fields arriving from all other scatterers. When the multiple scattering equations are averaged over all configurations of the scatterers, a hierarchy of solutions results relating the conditional average of the Green's function with n particles fixed to that with $n + 1$ particles fixed. The simplest solution lies in truncating this hierarchy at first order. This is known as the effective field approximation (EFA), also known as Foldy's approximation, and is equivalent to neglecting all correlations among the locations of scatterers [28]. The EFA is usually only valid for small particle densities. For higher volume fractions, the quasi-crystalline approximation (QCA) is a more appropriate formalism. It consists of a second-order truncation of the hierarchy, so two-particle correlations are included [28]. It permits the computation of the effective propagation constant of the wave, given the volume fraction, the complex dielectric of the spheres, the size parameter and the two-particle distribution function [29]. For spherical scatterers, the Percus–Yevick pair distribution function provides an adequate description of the positional correlation [30]. We perform computations of the QCA using Matlab routines available on the Internet [31]. The EFA result can be obtained by computing the QCA with the pair distribution function set equal to 1 [28].

Figure 3 shows a comparison of the experimental and theoretical reduced scattering coefficient μ_s' as a function of wavelength. These data span the range of size parameters from $ka \sim 1.6$ to 4.7, and show a variation in μ_s' by roughly a factor of 40 in magnitude. Typical error bars are shown, indicating the uncertainty associated with repeated measurements. The solid line shows the predictions of the QCA, calculated using parameters corresponding to those of the experiment. We have used an approximate form for the complex dielectric of

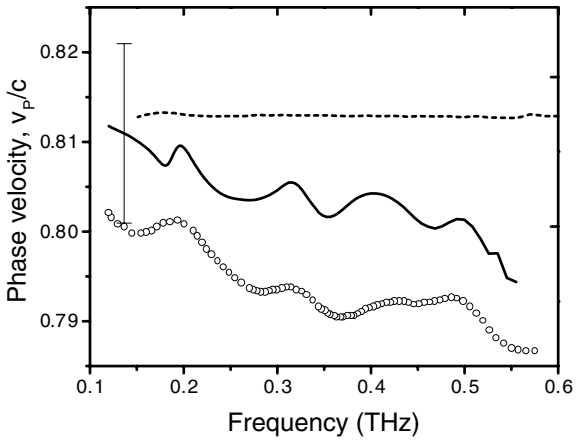

Figure 4. The open circles show the measured phase velocity, c/n_{eff}, as a function of frequency, extracted from the phases of the Fourier transforms of the time-domain waveforms. The dashed curve shows the prediction of the Maxwell–Garnett mixing formula, computed using experimentally measured values for the refractive index of solid teflon. The solid curve shows the prediction of the quasi-crystalline approximation. The error bar on this curve shows the uncertainty in the computed value arising from the $\pm 4\%$ uncertainty in the volume fraction of the spheres in the samples. Because the value of this input parameter is not determined with sufficient precision, it is not possible to conclude from these measurements if the discrepancy between the QCA and the data results from this uncertainty or from shortcomings in the theory.

the teflon spheres, obtained by fitting a low-order polynomial to the absorption coefficient reported by Birch *et al* [27]. Clearly, the theory underestimates the strength of the scattering, a result of neglecting higher-order correlations. Even so, the correspondence between the resonant features in the two curves is quite good.

The effects of multiple scattering can also be seen in the velocity of the transmitted radiation. The effective refractive index determines the phase velocity, according to $v_{\text{P}} = c/n_{\text{eff}}$. Figure 4 shows the measured frequency-dependent phase velocity, in units of c. One can use any number of different mixing formulae for computing the effective index of a two-component medium. The most common of these is the Maxwell–Garnett rule [32], which is equivalent to the QCA in the low-frequency limit [28]. For the situation described here, the Maxwell–Garnett result, computed with experimentally determined values for the refractive index of teflon, is shown as a dashed line in figure 4. It is clear that the dispersion and resonant features in the experimental data are not reproduced by the mixing rule. The full QCA result is shown as a solid line in figure 4. As shown in figure 3, there is a systematic shift between these computed values and the measurements. This could arise from the uncertainty in the experimentally determined volume fraction, since the phase velocity is essentially linearly dependent on the volume fraction [28]. The error bar on the theoretical curve shows a typical range in the computed phase velocity resulting from this uncertainty; this range is of the same order as the discrepancy between the computation and the experiment. As a result, the discrepancy could be due to the uncertainty in the volume fraction, or to the inadequacy of the QCA at large volume fractions. In order to evaluate the accuracy of the QCA with respect to phase velocity, a more accurate method for experimentally determining the volume fraction will be required. However, despite the apparent discrepancy, it is interesting to note that the overall dispersive trend, as well as the resonant features in the spectrum, are both well reproduced by the QCA calculation.

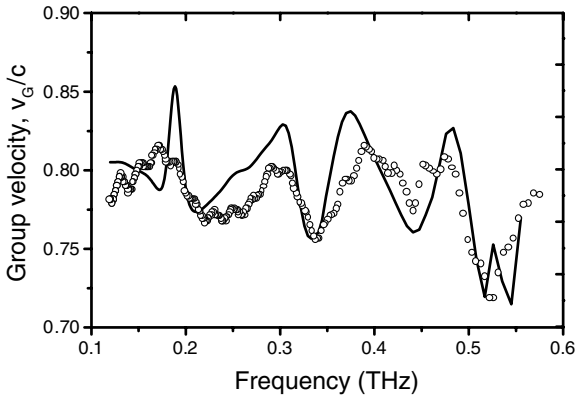

Figure 5. The open circles show the measured group velocity, obtained by numerically differentiating the measured effective index. The QCA prediction (solid curve) matches the data quite well.

Because these data are acquired with a broadband spectrometer, it is also possible to determine the effective group velocity. The group velocity of the wave depends not only on the effective index but also on its derivative, according to $v_G(\omega) = c\big/\big(n_{\text{eff}} + \omega\frac{\mathrm{d}n_{\text{eff}}}{\mathrm{d}\omega}\big)$. This is the velocity with which a wave packet moves through the medium. The group velocity is determined experimentally by numerically differentiating the measured effective index with respect to frequency. This is shown in figure 5, along with the QCA result (solid line). The agreement is much improved in comparison to figure 4, demonstrating that the QCA can be used to accurately compute group velocities even when the volume fraction is large enough so that the predicted phase velocity is less reliable.

4. Conclusions

We note that the QCA is generally assumed to be valid for volume fractions below ∼40%, whereas our measurements involve volume fractions exceeding 50%. In fact, the very high density regime (above 40%) has not been thoroughly investigated, so the validity of this second-order theory is not well established in this regime. Our results indicate that the QCA provides some indication of the scattering coefficient, and at least a reasonable estimate of the phase velocity of the wave. In the case of the group velocity, the agreement with the experiment is in fact quite good. Thus, while not perfect, the QCA is still useful even far beyond its expected limits of the validity. These results indicate the diminishing importance of higher-order correlations, at least in the case of moderate dielectric contrast studied here.

In conclusion, we have studied the propagation of terahertz pulses in a dense collection of spherical scatterers. The size of the scatterers corresponds to a size parameter $ka \sim 1$, in the Mie scattering regime. These experiments probe a regime of very high volume fraction, which has not been thoroughly explored previously, but which could be of relevance in the understanding of electromagnetic propagation in biomedical systems. We have modelled these results using the quasi-crystalline approximation, which accounts for two-particle correlations with the Percus–Yevick distribution function. The correspondence between theory and experiment is reasonable, considering the limitations of the QCA at high volume fractions. In future work, we intend to study similar problems using materials with higher dielectric contrast, which should display much more dramatic departures from the predictions of the theory.

Acknowledgment

This work has been supported in part by the United States National Science Foundation.

References

[1] Woolard D L 1997 Millimeter wave-induced vibrational modes in DNA as a possible alternative to animal tests to probe for carcinogenic mutations *J. Appl. Toxicol.* **17** 243–6
[2] Markelz A G, Roitberg A and Heilweil E J 2000 Pulsed terahertz spectroscopy of DNA, bovine serum albumin and collagen between 0.1 and 2.0 THz *Chem. Phys. Lett.* **320** 42–8
[3] Walther M, Fischer B, Schall M, Helm H and Jepsen P U 2000 Far-infrared vibrational spectra of all-trans, 9-cis and 13-cis retinal measured by THz time-domain spectroscopy *Chem. Phys. Lett.* **332** 389–95
[4] Mittleman D M, Gupta M, Neelamani R, Baraniuk R G, Rudd J V and Koch M 1999 Recent advances in terahertz imaging *Appl. Phys.* B **68** 1085–94
[5] Arnone D D, Ciesla C M, Corchia A, Egusa S, Pepper M, Chamberlain J, Bezant C, Linfield E H, Clothier R and Khammo N 1999 Applications of terahertz (THz) technology to medical imaging *Proc. SPIE* **3828** 209–19
[6] Han P Y, Cho G C and Zhang X-C 2000 Time-domain transillumination of biological tissues with terahertz pulses *Opt. Lett.* **25** 242–4
[7] Löffler T, Bauer T, Siebert K and Roskos H 2001 Terahertz dark-field imaging of biomedical tissue *Opt. Expr.* **9** 616–21
[8] Schumacher C R 1987 Electrodynamic similitude and physical scale modeling of nondispersive targets *J. Appl. Phys.* **62** 2616–25
[9] Cheville R A and Grischkowsky D 1995 Time domain terahertz impulse ranging studies *Appl. Phys. Lett.* **67** 1960–2
[10] Dorney T D, Johnson J L, Rudd J V, Baraniuk R G, Symes W W and Mittleman D M 2001 Terahertz reflection imaging using Kirchhoff migration *Opt. Lett.* **26** 1513–6
[11] Wang L, Ho P P and Alfano R R 1993 Time-resolved Fourier spectrum and imaging in highly scattering media *Appl. Opt.* **32** 5043–8
[12] Benaron D A and Stevenson D K 1993 Optical time-of-flight and absorbance imaging of biologic media *Science* **259** 1463–6
[13] Wang L, Ho P P, Liu C, Zhang G and Alfano R R 1991 Ballistic 2-D imaging through scattering walls using an ultrafast optical Kerr gate *Science* **253** 769–71
[14] O'Leary M, Boas D, Chance B and Yodh A 1995 Experimental images of heterogeneous turbid media by frequency-domain diffusing photon tomography *Opt. Lett.* **20** 426–9
[15] Popescu G and Dogariu A 2000 Ballistic attenuation of low-coherence optical fields *Appl. Opt.* **39** 4469-72
[16] Sebbah P, Pnini R and Genack A Z 2000 Field and intensity correlation in random media *Phys. Rev.* E **62** 7348–52
[17] Petoukhova A L, Steenbergen W and de Mul F F M 2001 Path-length distribution and path-length-resolved Doppler measurements of multiply scattered photons by use of low-coherence interferometry *Opt. Lett.* **26** 1492–4
[18] Schotland J C and Markel V A 2001 Inverse scattering with diffusing waves *J. Opt. Soc. Am.* A **18** 2767–77
[19] Ishimaru A and Kuga Y 1982 Attenuation constant of a coherent field in a dense distribution of particles *J. Opt. Soc. Am.* **72** 1317–20
[20] Nanbu Y and Tateiba M 1996 A comparative study of the effective dielectric constant of a medium containing randomly distributed dielectric spheres embedded in a homogeneous background medium *Waves Random Media* **6** 347–60
[21] Kuga Y, Rice D and West R D 1996 Propagation constant and the velocity of the coherent wave in a dense strongly scattering medium *IEEE Trans. Antennas Propag.* **44** 326–32
[22] Popescu C and Dogariu A 1997 Optical path-length spectroscopy of wave propagation in random media *Opt. Lett.* **24** 442–4
[23] Brodsky A, Shelley P, Thurber S R and Burgess L W 1997 Low-coherence interferometry of particles distributed in dielectric medium *J. Opt. Soc. Am.* A **14** 2263–8
[24] Pearce J and Mittleman D 2001 Propagation of single-cycle terahertz pulses in random media *Opt. Lett.* **26** 2002–4
[25] Jepsen P U, Jacobsen R H and Keiding S R 1996 Generation and detection of terahertz pulses from biased semiconductor antennas *J. Opt. Soc. Am.* B **13** 2424–36
[26] Mittleman D M, Jacobsen R H and Nuss M C 1996 T-ray imaging *IEEE J. Sel. Top. Quantum Electron.* **2** 679–92

[27] Birch J R, Dromey J D and Lesurf J 1981 The optical constants of some common low-loss polymers between 4 and 40 cm^{-1} *Infrared Phys.* **21** 225–8
[28] Tsang L, Kong J A and Shin R T 1985 *Theory of Microwave Remote Sensing* (New York: Wiley)
[29] West R, Gibbs D, Tsang L and Fung A K 1994 Comparison of optical scattering experiments and the quasi-crystalline approximation for dense media *J. Opt. Soc. Am.* A **11** 1854–8
[30] Tsang L, Kong J A and Habashy T 1982 Multiple scattering of acoustic waves by random distribution of discrete spherical scatterers with the quasicrystalline and Percus–Yevick approximation *J. Acoust. Soc. Am.* **71** 552–8
[31] Kong J 2001 Electromagnetic Wave MATLAB Library, Center for Electromagnetic Theory and Applications, Massachusetts Institute of Technology (webpage http://www.emwave.com)
[32] Mishchenko M I, Hovenier J W and Travis L D 2002 *Light Scattering by Nonspherical Particles* (San Diego, CA: Academic)